

Modeling Of A Diffraction Grating Coupled Waveguide Based Biosensor For Microfluidic Applications

Yixuan Wu*¹, Mark L. Adams¹

¹Auburn University

*yzw0040@auburn.edu

Abstract: A diffraction grating coupled waveguide based biosensor for microfluidic analysis is presented. The sensor is composed of optical elements, a flow cell with medium, and a binding layer that is formed on the dielectric slab of optical elements. COMSOL Multiphysics® is used to simulate the biosensor by measuring the refractive index of the binding layer. The modeling results show the high sensitivity of the device for measuring the change in refractive index.

Keywords: Biosensor, refractive index, grating coupler, waveguide.

1. Introduction

A biosensor is an analytical device which can detect and identify chemical or biological analytes by converting the biological or chemical signals into electrical or optical signals. Biosensors are widely used for applications in health such as glucose monitoring and pregnancy tests [1]. A label free biosensor is a technology that senses the analyte of interest without introducing a secondary transduction mechanism such as a fluorescent molecule. The biosensor can provide reliable information related to the components of the analyte in real time. Label free optical biosensing is a powerful method to detect biological elements as the sensing mechanism does not affect the structure of the analyte. One of the most common label free techniques measures the change of the refractive index (RI) [2]. When RI is modified by the analyte of interest, a change in the measured spectrum of the biosensor will be observed. The sensitivity of the biosensor is directly correlated to the spectrum change observed.

Grating couplers are a common optical component for introducing light into on-chip photonic structures. They are used extensively for optical interconnects and optical device integration. Grating couplers were presented initially by Dakss [3], and have been used for many other applications including biosensing [4, 5]. In this paper, a novel microfluidic diffraction

grating coupled waveguide (MDGCW) based biosensor is presented.

The MDGCW based biosensor has the following advantages: easy experimental integration, cost effective fabrication, and relatively high sensitivity. Most diffraction grating based biosensors use the binding reaction of the analyte on the patterned surface of the grating coupler, which changes the effective refractive index of the coupler. Either the coupling angle of the incident light is varied to find the peak intensity of the reflected light [6, 7], or a static angle is chosen and the reflected intensity is measured [8]. Unlike sensors where the binding occurs on the grating, in our MDGCW based biosensor the binding occurs on the dielectric slab of the optical elements similar to research presented in [9]. The dielectric slab forms a capping layer for a microfluidic channel through which the analyte of interest is introduced to the device. The grating itself and the sensitivity of the biosensor depends on the peak shift in the light spectrum. This technique allows for simple fabrication and an unobstructed light path to the grating. Moreover, the binding layer under the grating will not influence the patterned structure of the grating coupler and can simplify analysis. COMSOL Multiphysics® is used to model MDGCW based biosensor and the results are shown in this paper.

2. Theory

A classical optical grating structure is made of periodic slits in an opaque medium. Each slit is regarded as an independent source of light which will interfere with each other to generate the classical diffraction pattern known from geometric optics. Figure 1 illustrates the typical grating effect.

Mathematically this effect can be described by the general grating equation for reflection and transmission:

$$d(\sin\phi_t - \sin\phi_i) = m\lambda \quad (1)$$

where d is grating period, m is diffraction order, λ

is the wavelength of the light, φ_i is the incidence angle and φ_t is the angle of m^{th} diffraction order.

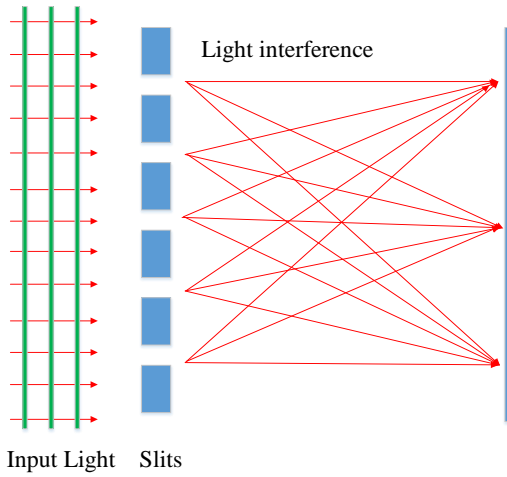


Figure 1. Principle of a classical optical grating.

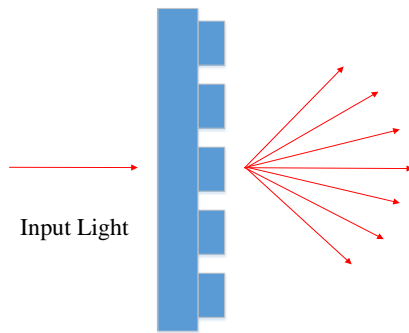


Figure 2. Light incident onto a binary grating will be diffracted to several diffraction orders.

A binary grating, shown in Figure 2, is used as the basic coupling structure. A phase grating consists of an array of narrow ridges of alternating refractive indices and the binary grating is a kind of phase grating with periodic thin rectangular ridges [10]. The binary grating can be mathematically described by:

$$d(n_t \sin \varphi_t - n_i \sin \varphi_i) = m\lambda \quad (2)$$

where n_t is the refractive index of the transmitted medium and n_i is the refractive index of the incidence medium.

The grating equation (2) can be used to calculate the parameters of the binary grating coupler. The difference between the classical diffraction grating and the binary grating is that

the light passes through two different media. For the MDGCW based biosensor, the same method can be used to describe the grating coupler [10]. The following equations can be used to extend equation (2) to accurately predict the coupling parameters:

$$n_{eff} = n_t \sin \varphi_t \quad (3)$$

$$n_{eff} = n_{top} * \sin \varphi_i + m \frac{\lambda}{d} \quad (4)$$

Then the equation for the biosensor can be described as:

$$\Delta n_{eff} = n_{top} * \sin \varphi_i + m \frac{\Delta \lambda}{d} \quad (5)$$

where n_{eff} is the effective refractive index of the light coupled into the grating coupler, n_{top} is the refractive index of the material on the grating coupler.

The geometry of the MDGCW based biosensor is shown in Figure 3. The sensor consists of two grating couplers, a waveguide between the two grating couplers, a polydimethylsiloxane (PDMS) flow cell, and an aqueous medium containing a reagent of interest. The n_{eff} will change as a result of analyte binding to the substrate. From equation (4), when n_{top} and $\sin \varphi_i$ are constant, Δn_{eff} will influence the light coupled into the waveguide and cause a shift of the peak in the optical spectrum. The peak of the light coupled into the waveguide will be shifted linearly due to the change of n_{eff} . For a certain wavelength, changing n_{eff} will change the propagation mode in the waveguide.

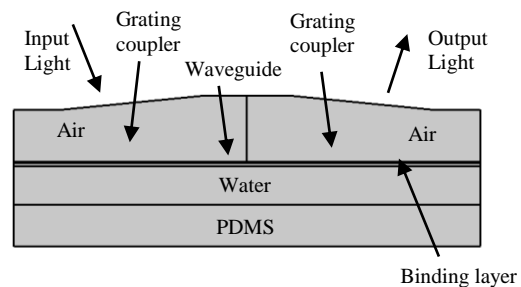


Figure 3. Geometry of the microfluidic diffraction grating coupled waveguide based biosensor

Furthermore, n_{eff} can be calculated by effective index techniques or numerical methods [11]. For both solutions, n_{eff} is related to the normalized frequency, propagation parameter, and asymmetry parameters of the structure. These parameters depend on the wavelength of the light, the dimension of the structure, and the refractive index of the media. So the refractive index of the binding layer and the dimension of the binding layer will affect n_{eff} and the light coupled into the waveguide.

When the RI of the binding layer is changed to different values, the peak shift in the spectrum will be linearly proportional to the change of the refractive index. The peak shift is related to the sensitivity of the biosensor. So the sensitivity can be obtained by the following:

$$S = \frac{\Delta\lambda}{\Delta n} \quad (6)$$

If the coupling angle is changed, it will result in the peak shift at the spectrum and it will not affect n_{eff} and other parameters. Given equations (2-6), a structure can be designed to optimize the biosensor performance.

For the model, the optimized grating layer is shown in Figure 4. The RI of the grating and waveguide is 2. Beneath the grating, there is a 200nm binding layer, a 3 μ m water layer and a 3 μ m PDMS layer. The 100nm thick grating coupler consisted of 17 grating periods with a 650nm period, a 50% fill-factor, and an etch depth of 80nm. The top of the MDGCW is exposed to air and the light is incident input from the upper left of the air and output from upper right of the air. The length of the waveguide between the two gratings is flexible, and can be adjusted to maximize the interaction length between the binding agent and analyte of interest. Due to the first grating, the incident light is reflected and transmitted into several diffraction orders, and a fraction of the light will be coupled into the waveguide. Between the input and output gratings, the light will propagate through the waveguide. The waveguide is surrounded by air and the binding layer and it can be modeled as a dielectric slab waveguide [12]. The guided electric field will be confined in the waveguide and will be decayed exponentially in the air and the binding layer. The light coupled into the waveguide will propagate to the second grating.

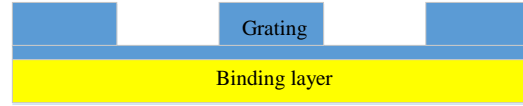


Figure 4. Details of the grating design and binding layer.

With the help of the second grating, the light will be reflected and transmitted into several diffraction orders again and part of the light will be diffracted out for detection. Both the intensity and wavelength of the output light can be measured to determine the sensitivity of the biosensor.

3. Use of COMSOL Multiphysics®

The COMSOL Multiphysics® Wave Optics module was used to simulate the change in refractive index induced by the binding of reagent to the substrate of the optical element. The model used COMSOL's boundary mode analysis. The light was excited at the upper left side of the air and the transmitted power is detected at the upper right side of the air, as shown in Figure 5. The light propagates in the waveguide between two grating couplers as shown in Figure 6. A parametric sweep was used to excite different wavelengths of the incident light and scattering boundary conditions were used to reduce the reflection from the boundary. A boundary mode analysis was performed to solve for the propagation constant. Moreover, to make the simulation accurate, mesh refinement studies were used to determine the optimum element size for the mesh. The electric field and propagation constant can be obtained by the follow equations:

$$\nabla \times \mu_r^{-1}(\nabla \times E) - k_0^2 \left(\epsilon_r - \frac{j\sigma}{\omega\epsilon_0} \right) E = 0 \quad (7)$$

$$\lambda = -j\beta - \delta_z \quad (8)$$

$$E(x, y, z) = \tilde{E}(x, y)e^{-ik_z z} \quad (9)$$

where β is the propagation constant, δ_z is the damping along the propagation direction. Equation (7) is the eigenfunction to define the eigenvalue β and to solve the electric field and magnetic field.

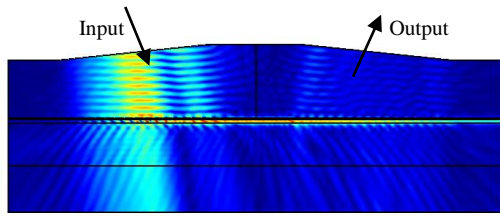


Figure 5. Electric field distribution of the diffraction grating coupled waveguide based biosensor

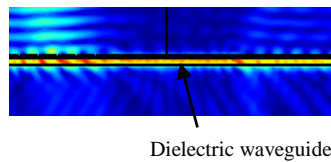


Figure 6. Electric field distribution in the waveguide of the sensor.

4. Results

Model results indicated good device sensitivity for measurement of the refractive index of the binding layer. Figure 7 illustrates the modeling results for the following parameters: $n_g = 2$, $n_{bl} = 1.6, 1.65, 1.7, 1.75$, where n_g and n_{bl} are the refractive indices of the grating and binding layer, respectively. The RI of water is set to 1.33, the RI of air is set to 1 and the RI of PDMS is set to 1.41. The binding layer thickness was set to $0.2\mu\text{m}$ and the coupling angle was 5.7° . The incident wavelength spanned $0.87\mu\text{m}$ to $0.97\mu\text{m}$. The sensitivity was calculated to be 387nm per refractive index unit. The peak intensity was between 3.5% and 5%, due to the coupling efficiency of the diffraction gratings and propagation losses in the waveguide. Although the reduction in intensity is significant, enough light should exit the biosensor to measure the peak shift.

Additional simulations were performed where the coupling angle was changed while maintaining the other parameters of interest. Coupling angles of 7.9° and 10.1° were chosen for simulation to determine the sensitivity of the biosensor to incidence angle. Figures 8 and 9 illustrate the simulation results for these two angles respectively. Simulations showed that an increasing incidence angle resulted in a blue-shifted peak and lower sensitivity.

Finally, simulations were performed where the thickness of the binding layer was changed while other parameters remain unchanged. The binding layer thickness impacts the effective refractive index. The thickness of the binding layer was set to $0.1\mu\text{m}$ and $0.15\mu\text{m}$ respectively, as seen in figures 10 and 11. From the simulation results, it can be seen that the sensitivity of $0.15\mu\text{m}$ is close to the sensitivity of $0.2\mu\text{m}$, but the sensitivity of $0.1\mu\text{m}$ is much smaller in comparison with the sensitivity of $0.2\mu\text{m}$. Figure 12 illustrates a comparison of the different incident angles for $n_{bl} = 1.7$.

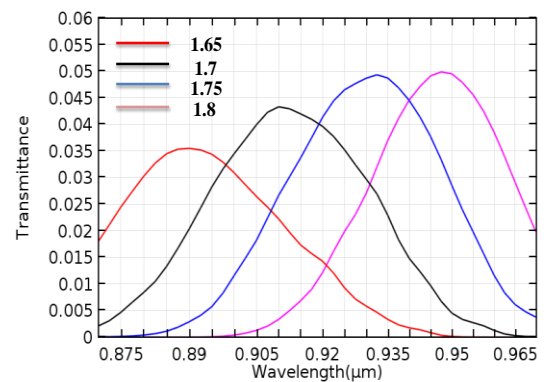


Figure 7. Spectrum when binding layer is $0.2\mu\text{m}$ and coupling angle is 5.7° .

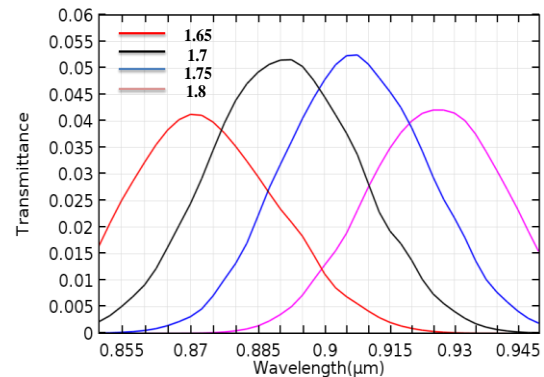


Figure 8. Spectrum when binding layer is $0.2\mu\text{m}$ and coupling angle is 7.9° .

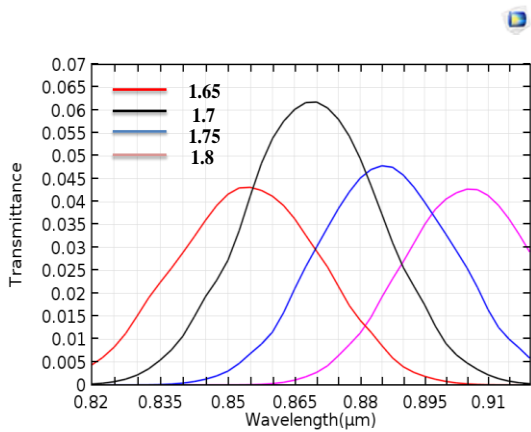


Figure 9. Spectrum when binding layer is $0.2\mu\text{m}$ and coupling angle is 10.1° .

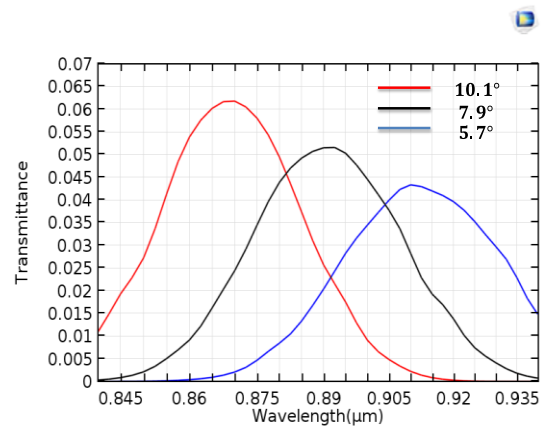


Figure 12. Spectrum when binding layer is $0.2\mu\text{m}$ and the refractive index of the binding layer is 1.7.

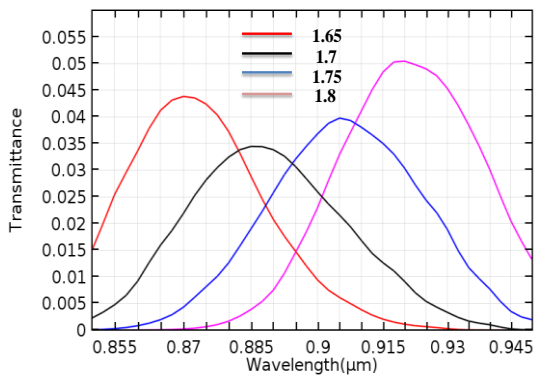


Figure 10. Spectrum when binding layer is $0.15\mu\text{m}$ and coupling angle is 5.7° .

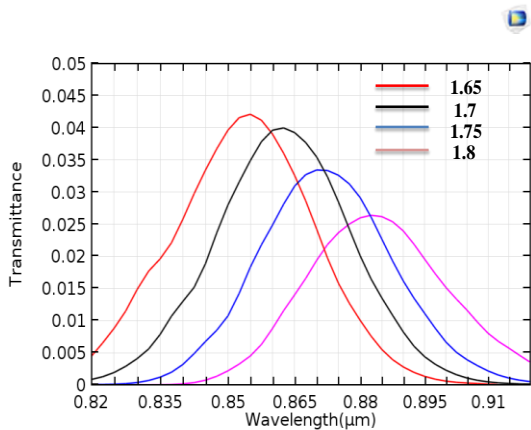


Figure 11. Spectrum when binding layer is $0.1\mu\text{m}$ and coupling angle is 5.7° .

5. Conclusions

A microfluidic diffraction grating coupled waveguide based biosensor which measures the refractive index of the binding layer under the grating was presented. Simulation results have shown that the MDGCW based biosensor should have good sensitivity. As expected, the resulting sensitivity was affected by the refractive index of the binding layer, the dimension of the binding layer, and the coupling angle of the incident light.

The biosensor presented should allow for easy fabrication and an unobstructed light path to the grating. Moreover, since the binding layer is located on the grating substrate, it will not influence the actual patterned structure of the grating coupler. Furthermore, since the effective refractive index of the grating is related to the grating period, the thickness of the grating, and the etch depth of the grating, changes to any of these parameters allow further optimization of the MDGCW based biosensor.

6. References

1. H. Mukundan et al., Waveguide-Based Biosensors for Pathogen Detection, *Sensors*, **9**, 5783- 5809 (2009)
2. Y. Guo et al, Optofluidic Fabry-Pérot cavity biosensor with integrated flow-through micro-/nanochannels, *Applied Physics Letters*, **98**, 041104 (2011)

3. M. L. Dakss et al., Grating Coupler for Efficient Excitation of Optical Guided Waves in Thin Films," *Appl. Phys.Lett*, **16**, 523-525 (1970)
4. N. Darwish et al., Multi-analytic grating coupler biosensor for differential binding analysis, *Sensors and Actuators B*, **144**, 413–417 (2010)
5. D. Duval et al., Grating Couplers Integrated on Mach–Zehnder Interferometric Biosensors Operating in the Visible Range, *IEEE Photonics Journal*, **5**, 3700108-3700108 (2013)
6. J. Vörös et al., Optical grating coupler biosensors, *Biomaterials*, **23**, 3699-3710 (2002)
7. X. Wei and S. M. Weiss, Guided mode biosensor based on grating coupled porous silicon waveguide, *Opt. Exp.*, **19**, 11330-11339 (2011)
8. Z. Lai et al., Label-free biosensor by protein grating coupler on planar optical waveguides, *Opt. Lett.*, **33**, 1735-1737 (2008)
9. P. Kozma et al., Grating coupled optical waveguide interferometer for label-free biosensing, *Sen. and Act. B*, **155**, 446–450 (2011)
10. K. R. Harper, Theory, Design, and Fabrication of Diffractive Grating Coupler for Slab Waveguide, Masters Dissertation, Brigham Young University (2003)
11. L.A. Colden and S.W. Corzine, Diode Lasers and Photonic Integrated Circuits, 322-327, John Wiley&Sons, Canada (1995)
12. K. Okamoto, Fundamentals of Optical Waveguides, 13-55, Academic press, USA (2010)